Spatial Coordination of Chloroplast and Plasma Membrane Activities in *Chara* Cells and Its Disruption through Inactivation of 14-3-3 Proteins

A. A. Bulychev[1]*, P. W. J. van den Wijngaard[2], and A. H. de Boer[2]

[1]*Department of Biophysics, Faculty of Biology, Lomonosov Moscow State University,*
119992 Moscow, Russia; fax: (7-095) 939-1115; E-mail: bulychev@biophys.msu.ru
[2]*Department of Developmental Genetics, Vrije Universiteit, Faculty of Earth and Life Sciences,*
De Boelelaan 1085, 1081 HV Amsterdam, The Netherlands; E-mail: ahdeboer@bio.vu.nl

Abstract—In *Chara corallina* cells exposed to continuous light, external pH (pH_o) and photosystem II (PSII) photochemical yield show correlated banding patterns. Photosynthetic activity is low in cell regions producing alkaline zones and high in the acid regions. We addressed the question whether (and how) photosynthetic activity and plasma membrane (PM) H^+-pumping and H^+-conductance are coupled in the different bands. First, PM H^+-pump activity was stimulated with fusicoccin. This resulted in a more acidic pH in the acid bands without disturbing the correlation of photosynthetic electron transport and H^+ fluxes across the PM. Next, H^+-pump activity was reduced through microinjection of a phosphorylated peptide matching the canonical 14-3-3 binding motif RSTpSTP in the acid cell region. Microinjection induced a rapid (~5 min) rise in pH_o by ca. 1.0 unit near the injection site, whereas the injection of the non-phosphorylated peptide had no effect. This pH rise confirms the supposed inhibition of the H^+-pump upon the detachment of 14-3-3 proteins from the H^+-ATPase. However, the PSII yield in the cell regions corresponding to the new alkaline peak remained high, which violated the normal inverse relations between the pH_o and PSII photochemical yield. We conclude that the injection of the competitive inhibitor of the H^+-ATPase disrupts the balanced operation of PM H^+-transport and photosynthetic electron flow and promotes electron flow through alternative pathways.

Key words: *Chara corallina*, plasma membrane H^+-pump, chlorophyll fluorescence, photosynthetic electron transport, 14-3-3 proteins, fusicoccin

It is well known that chloroplast functioning is closely related to ion fluxes at the plasma membrane (PM) [1, 2]. The induction of photosynthesis is accompanied by ion and metabolite transport across the chloroplast envelope, which influences the PM H^+-pump and the functional state of PM ionic channels [2-6]. For aqueous plants inhabiting slightly alkaline environments, the light-induced activation of the H^+-pump can be physiologically important because the local acidification near the cell surface shifts the HCO_3^-/CO_2 equilibrium to a higher content of CO_2 and provides the cell with a form of inorganic carbon that readily permeates the PM [7, 8]. These feedback relationships, including the promotion of photosynthesis by the available substrate, gain further interest in view of the spatial heterogeneity of photosynthetic activity and membrane transport processes. Spatial heterogeneity of photosynthetic metabolism was for example observed during the induction of photosynthesis in maize leaves [9]; the reasons for this heterogeneity remain unexplained and require close attention. An interesting model system is *Chara corallina* cells, where spatial heterogeneity of PM proton fluxes and photosynthetic activity develops from a homogeneous distribution upon a dark-light transition [10-12]. The longitudinal pH profiles recorded along the illuminated *Chara* internode comprise alternating acidic and alkaline bands. Measurements of chlorophyll fluorescence with pulse-amplitude-modulated fluorometry on small regions of a

chloroplast layer provided evidence that the photosynthetic activity in a single *Chara* cell is also subject to a banding pattern [13].

The mechanism of band emergence in *Chara* is not yet understood, but the pattern formation could be simulated with a reaction−diffusion model assuming a basically homogeneous spatial distribution of pumps and H^+-conducting pathways [12]. The model was based on the assumption that H^+-conductance is activated in the alkaline zones due to opening of high-pH channels or operation of H^+/HCO_3^- symport. It was also supposed that the pump-driven H^+ efflux in the PM depends on photosynthetic ATP production [1]. Such a homogeneous system was shown to become unstable at high light conditions and produce bands with spatially distributed active H^+-pumps and leaks. One hypothesis to explain the banding pattern is that the acid and alkaline zones originate from differential ATP-synthesizing capacity in chloroplasts in different regions of the cell. In those regions where the transmembrane proton gradient in the chloroplast thylakoids is not readily utilized for ATP synthesis, higher amounts of protons accumulate in the thylakoid lumen, thus restricting the photosynthetic electron flow (photosynthetic control) [14]. The high H^+ uptake by thylakoids would be reflected in lowering the H^+ concentration in the chloroplast stroma and the cytoplasm [15]. The lowering of the H^+ concentration (more alkaline pH) in the cytoplasm is thought to suppress the activity of the PM H^+-pump, cause local alkalization of the medium, and activate the supposed high-pH channels [16, 17]. This will further increase pH_o, diminish the amount of available CO_2, and suppress the linear electron flow providing NADPH to the Calvin cycle. Conversely, in the regions where chloroplasts rapidly produce ATP and the cytoplasmic ATP pool supports the H^+-pump, alkalization is prevented and a band with acid pH_o develops. This elevates the amount of CO_2, which readily permeates through the membrane and ensures high photosynthetic rates.

Clearly, further efforts are needed to elucidate interactions between the chloroplast and the PM activities that give rise to the pH banding pattern. In this context, the effects of H^+-pump modulators on spatial distribution of PM H^+ fluxes and photosynthetic activity are of interest. In plant cells both the catalytic and transport activity of the PM H^+-pump are controlled by phosphorylation-dependent interaction with 14-3-3 proteins [18, 19]. The 14-3-3 proteins are involved in signaling pathways and act as adapters, chaperones, activators, and repressors [20, 21]. Interaction with target proteins occurs in a sequence- and phosphorylation-dependent fashion; canonical sequences having the form RSXpSXP or RX(Y/F)XpSXP, where pS indicates a phosphorylated serine residue [22]. However, the H^+-ATPase is a notable exception with a tripeptide 14-3-3 interaction motif located at the extreme end of the C-terminus with the sequence YpTV, where pT

is a phosphorylated threonine residue [23]. This C-terminus acts as an autoinhibitor, and phosphorylation of the threonine residue followed by 14-3-3 binding leads to displacement of the autoinhibitory domain and thus activation of the H^+-ATPase. This mechanism was very nicely shown for the blue light induced activation of the PM H^+-ATPase in stomatal guard cells [24, 25].

Interaction between 14-3-3 and target proteins can be broken by competitive binding of phosphoserine peptides that match the canonical binding sequences in 14-3-3 target proteins [26, 27]. In plants, a phospho-peptide matching the 14-3-3 interaction domain in barley nitrate reductase (NR), containing a phosphorylated (pS) motif (RSTpSTP), successfully prevented 14-3-3 inhibition of the chloroplast F_0F_1-synthase [28] and activation of PM K^+-channels [29]. We expect that introduction of the NR-peptide into the cytoplasm will inhibit the ATP-dependent H^+-pump in a competitive manner through binding to endogenous 14-3-3. In this manner, we want to test whether the intracellular microinjection of this peptide can be used as a tool for disrupting normal interactions between the chloroplasts and the plasma membrane. On the other hand, the PM H^+-pump can be activated by fusicoccin (a phytotoxin from the parasitic fungus *Fusicoccum amigdali*) through the interaction of fusicoccin with a complex of 14-3-3 protein and the C-terminus of the H^+-ATPase. Thus, the role of the PM H^+-pump in coordination of photosynthetic activity and proton fluxes at the PM can be assessed through both inhibition and activation of the H^+-ATPase.

MATERIALS AND METHODS

Detection of alkaline and acidic bands in *Chara* cells. The Characean alga *Chara corallina* Klein ex Willd. were grown in an aquarium under laboratory conditions (scattered daylight, 20-22°C). Internodal cells about 6 cm in length and 0.8-1 mm in diameter without apparent calcium depositions were excised from a strand and placed in artificial pond water containing 0.1 mM KCl, 1.0 mM NaCl, and 0.1 mM $CaCl_2$ (pH 6.8-7.2).

A transparent chamber accommodating a *Chara* internode was mounted on the stage of an Axiovert-25 inverted microscope (Carl Zeiss, Germany) equipped with a Microscopy-PAM (Walz, Germany) fluorometric unit. Measurements of local pH and chlorophyll fluorescence were performed as previously described [13]. The alkaline and acidic bands were detected with glass-insulated antimony pH microelectrodes having a tip diameter of 10-50 μm. The terms "alkaline and acidic cell regions" designate the cell parts adjacent to alkaline and acidic zones of the outer media, respectively.

Chlorophyll fluorescence measurements. Chlorophyll fluorescence was measured on small portions of a chloroplast layer (a circular area of 100 μm in diameter) with a

Microscopy-PAM fluorometer (Walz). Characteristics and features of Microscopy-PAM are described in detail by Goh et al. [30]. The objective lens was focused on a chloroplast layer in the lower cell side. The high sensitivity of the Microscopy PAM fluorometer permitted the use of low-intensity measuring light that had no actinic effect. The lack of actinic effect was evidenced by high ratios of variable fluorescence to maximum fluorescence yield ($\Delta F/F_\mathrm{m}$), approaching their upper limit in dark-adapted cells.

Actinic blue light was directed to the cell from above. The light from a halogen lamp of the upper light source of an Axiovert 25 microscope passed through a SZS-22 blue glass filter ($\lambda < 580$ nm). The light intensity at the cell level was about 20 μmol/sec per m^2 (up to 30 μmol/sec per m^2 in some experiments). The PSII effective yield in cells exposed to actinic light was estimated from the equation:

$$\Delta F/F_\mathrm{m}' = (F_\mathrm{m}' - F)/F_\mathrm{m}',$$

where F_m' is the maximum fluorescence yield obtained under a saturation pulse superimposed on the actinic (and measuring) light, and F is the actual fluorescence yield measured under actinic light.

Microinjection procedure. A phospho-peptide (NR-P) matching the 14-3-3 interaction domain in barley nitrate reductase (NR) containing a phosphorylated (pS) motif (RSTpSTP) has been used in these experiments. A non-phosphorylated peptide served as a control (NR-C). The peptide samples (1.2 and 1.1 mg, respectively) were dissolved in 100 μl of 50 mM KCl. The pipettes for microinjection were pulled from Pyrex glass capillaries. The tip was stubbed under an angle of about 45° to reduce resistance to liquid flow. The tip dimension was about 5 μm. The pipette was fixed in a sealed holder with an outlet connected to a microinjector unit (Biopribor, Pushchino, Russia). Prior to use the pipette tip was filled with light oil and then a portion of the peptide solution was sucked into the pipette shank to a length of 1 mm. According to estimates based on the pipette taper geometry, the sample volume constituted about $7 \cdot 10^5$ μm^3 ($7 \cdot 10^{-4}$ μl) and contained approximately $8 \cdot 10^{-3}$ μg of the peptide. After the pipette insertion, pressure was applied to the pipette in order to ensure the microinjection. The microinjection was performed on normally turgescent cells. The injection lasted for 5-10 min, until the approach of oil–water boundary to the pipette tip. In some cases, the oil droplet was ejected at the end of the microinjection procedure. The microinjection had no immediate effect on cytoplasmic streaming, which served as an indicator of cell viability. When the amount of $8 \cdot 10^{-3}$ μg peptide is uniformly distributed over a cylindrical cytoplasmic layer of *C. corallina* internode (volume ~3.8 μl) the peptide concentration in the cytoplasm would be about $2 \cdot 10^{-3}$ g/liter, which is roughly equivalent

to 1 μM. The local concentration could be substantially higher due to non-uniform distribution of the injected sample. The bulk of liquid introduced during pressure injection first remains in a cytosolic sac near the injection site. The use of fluorescent dyes allows visualization of loading and spreading of the injected substances over the cell. Such observations show that the distribution of injected substances within the cell remains incompletely uniform for hours after the injection, despite the ongoing cytoplasmic streaming. The minimum final concentration is determined by the distribution of the peptide over the total cell volume, which is approximately 10 times larger than the cytoplasmic volume. After puncturing the cell, pH$_\mathrm{o}$ was measured near the injection site (at a distance of 0.3-0.4 mm).

Prior to and following the microinjection, the $\Delta F/F_\mathrm{m}'$ and pH$_\mathrm{o}$ profiles were repeatedly measured at 30- to 50-min intervals for a period of 3-5 h. Records were made on the middle cell part measuring 15-20 mm. Experiments were performed in four replicates on different cells. The data in figures display the results of representative experiments, with mean values and standard errors obtained for replicate measurements.

RESULTS AND DISCUSSION

Correlation of $\Delta F/F_\mathrm{m}'$ and plasma membrane H$^+$ transport in untreated and fusicoccin-treated cells. Figure 1 shows the longitudinal profiles of pH$_\mathrm{o}$ and the effective quantum yield of PSII ($\Delta F/F_\mathrm{m}'$) that were measured along a 15-mm segment of an untreated *Chara corallina* cell
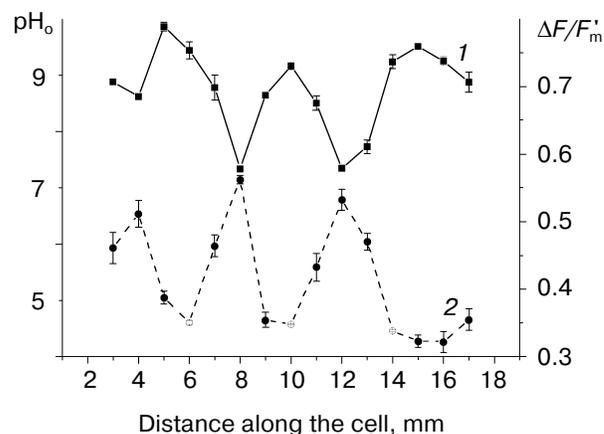
Fig. 1. Longitudinal profiles of pH near cell surface (*1*) and the effective quantum yield of PSII ($\Delta F/F_\mathrm{m}'$) (*2*) in an untreated *Chara corallina* cell exposed to continuous blue light (20 μmol/sec per m^2). Data represent mean values and standard errors for three replicate measurements performed within 2.5-h period on the central part of a whole cell. In this and other figures, the reference (zero) point of distance along the cell was chosen arbitrarily.

exposed to continuous light. The patterns of $\Delta F/F'_m$ and H^+ transport across the PM showed a remarkable correspondence. The effective quantum yield of PSII activity was low in the high pH regions (alkaline zones) and was high in the acidic zones.

A recent finding that alkaline zones are induced in *Chara* cells when the chloroplasts are moved away from the targeted area [31] provide indirect evidence in support of the low photosynthetic activity of chloroplasts in the alkaline cell regions. An important question is whether there is a causal coupling between the pH-banding pattern and the PSII photochemical yield, or whether they can be changed independently. To address this question, we first examined the effect of fusicoccin, a well-known

activator of PM H^+-ATPase, on the profiles of pH_o and $\Delta F/F'_m$. Fusicoccin was added to the external medium at concentrations from 6 to 10 μM in various experiments. Figure 2a shows that fusicoccin stimulated H^+ extrusion in acidic zones, in line with numerous reports that fusicoccin is a potent activator of plasma membrane H^+-pump activity in higher plant cells [32]. Note that the pH in the alkaline bands was not affected. The fusicoccin treatment enhanced the quantum yield, indicative of non-cyclic electron transport rate, particularly in the acidic cell regions (Fig. 2b). This is in stark contrast with a recent report that in stomatal guard cells fusicoccin strongly suppressed the photosynthetic electron transport activity [2, 30]. This stronger coupling between pH bands and PSII activity peaks (Fig. 2) is in line with the original model that CO_2 availability increases with H^+-pump activity and that PSII activity shows peaks where the CO_2 concentration is high.

Induction of a new alkaline band upon microinjection of NR-P peptide. In an attempt to suppress the H^+-pump activity, the NR-P and NR-C peptides were injected. We anticipated that NR-P might inhibit the PM H^+-pump through competition for 14-3-3 binding and wondered if this inhibition would affect the photosynthetic electron transport through depletion of the substrate CO_2. Figure 3 shows pH_o changes (average of four independent measurements) induced by the injection of each peptide into an acidic region of a *C. corallina* cell. Prior to microinjection, steady-state pH_o and $\Delta F/F'_m$ profiles, similar to that shown in Fig. 1, were measured. The pipette insertion was accompanied by a transient short-term pH change, which presumably reflects the leak of protons through the region of an unsealed pipette−membrane contact; these changes were not considered meaningful.

The major difference between the pH_o recordings after the injections of NR-P and NR-C is that the injection of NR-P was followed by an increase in pH_o within several minutes from 7.0-7.2 to 8.0-8.75 in various experiments (Fig. 3a), whereas injection of NR-C induced no significant pH rise (Fig. 3b). This rapid alkalization of a normally acidic region induced by microinjection of NR-P and the lack of such alkalization after the injection of NR-C suggests that the phosphorylated peptide transfers the PM H^+-ATPase to the inactive state because it competes with the pump for binding to 14-3-3 proteins [21]. This is probably the first demonstration of the sensitivity of the H^+-pump to 14-3-3 proteins *in vivo*. Clearly, the increase in pH_o upon NR-P injection arises not from the pipette insertion *per se* or mechanical stimulation by the injected volume of saline. The alkalization region was confined to a few millimeters around the microinjection point.

NR-P injection disrupts correlation of pH_o and $\Delta F/F'_m$ spatial profiles. Next, we monitored the profiles of pH_o and $\Delta F/F'_m$ before (Fig. 4a) and during several hours after injection with NR-P (Figs. 4b and 4c). Before injection,
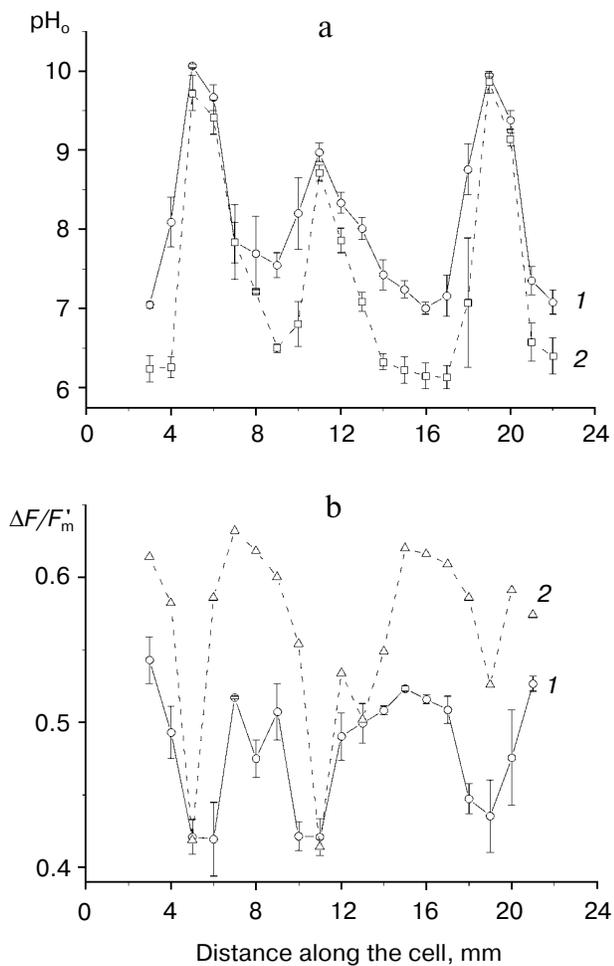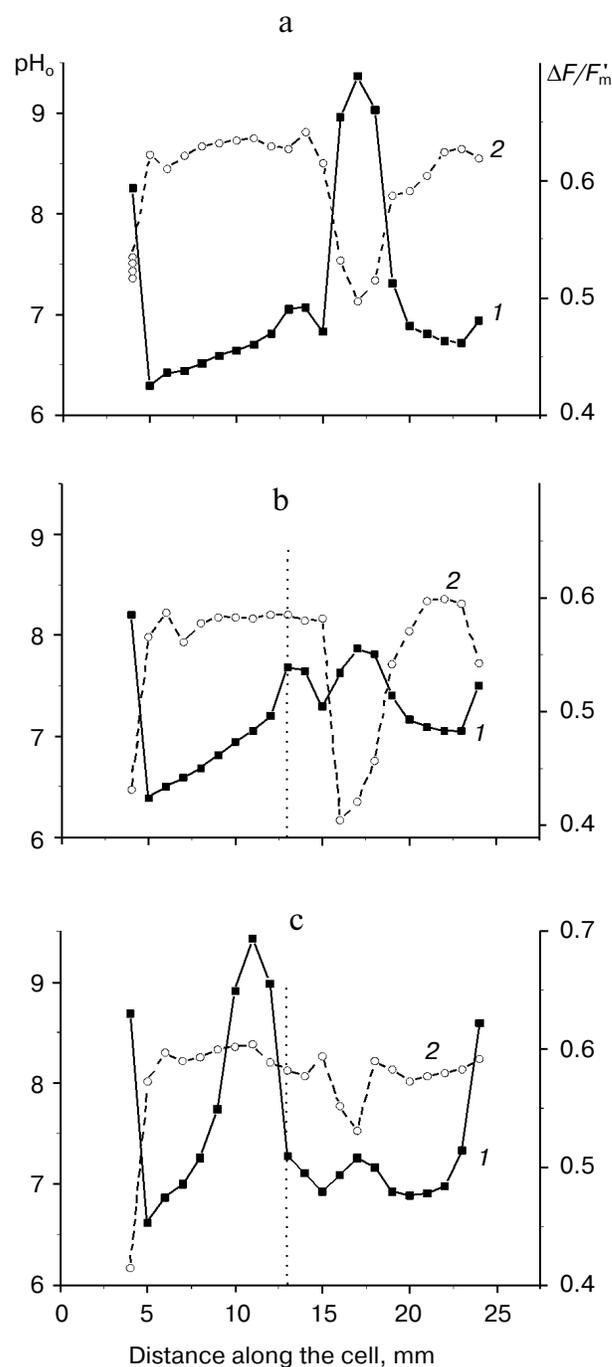
Fig. 2. Effect of fusicoccin (FC, 10 μM) on longitudinal profiles of pH_o (a) and $\Delta F/F'_m$ (b). Solid lines represent pH_o and $\Delta F/F'_m$ profiles for the untreated cells (artificial pond water) (*1*), and dashed lines correspond to the fusicoccin treatment (*2*). Bars indicate standard errors for three replicate measurements performed within 3 h before FC addition and for two replicate measurements obtained within 2 h after FC addition. The $\Delta F/F'_m$ profile in the fusicoccin-treated cells (b) was measured 2 h after the fusicoccin addition.
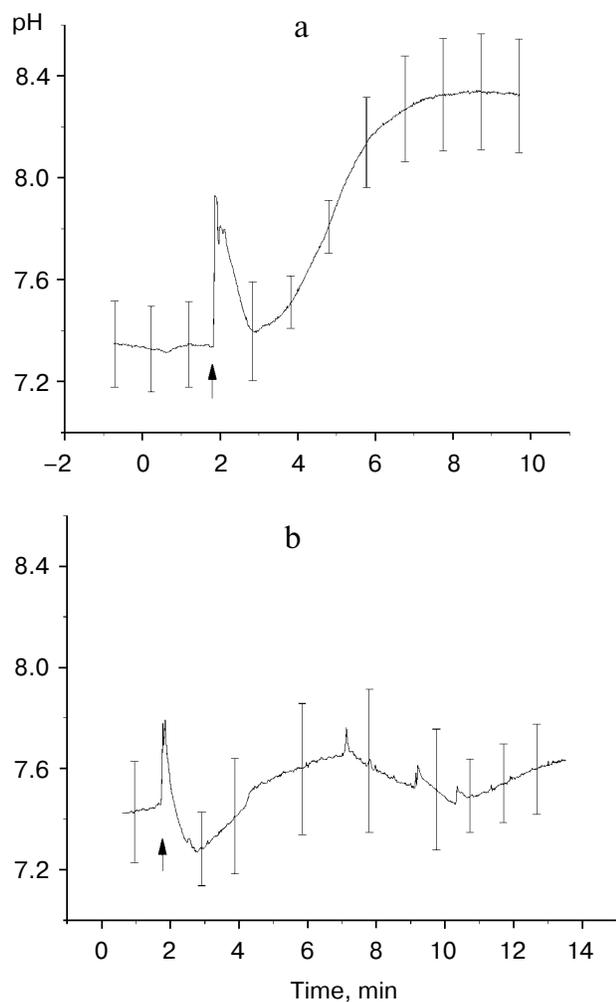
Fig. 3. Changes in pH near the surface of a *C. corallina* cell caused by the microinjection of the NR-P peptide (a) containing a phosphorylated (pS) motif (RSTpSTP) and of a similar non-phosphorylated peptide (NR-C) (b). Solid lines were obtained by averaging four experimental records for each treatment; bars represent standard errors of the means. Upward arrows indicate the moment when the micropipette was inserted. Secondary smaller jumps on record (b) were caused by extra pressure applied to the pipette.

Fig. 4. Disturbance of the pH_o (*1*) and $\Delta F/F_m'$ (*2*) spatial patterns after the intracellular microinjection of NR-P phosphorylated peptide (at the region marked with dotted vertical line) to a final concentration of about 10^{-6} M. a) Prior to microinjection, the pH_o and $\Delta F/F_m'$ profiles are correlated: $\Delta F/F_m'$ was low in the alkaline band (peak at 17 mm) and high in the acidic region. b) One hour after the NR-P microinjection, a new alkaline band appeared at the place of microinjection, but $\Delta F/F_m'$ remained high in this band. c) Three hours after the microinjection of NR-P, the new alkaline band had shifted (peak at 11 mm) but, unlike the control situation, $\Delta F/F_m'$ remained high in this band.

two alkaline regions were observed over a length of 20 mm in one of the experiments (Fig. 4a). The $\Delta F/F_m'$ pattern largely corresponded to the pH pattern. One hour after the injection of NR-P (injection position marked with a dotted straight line), a new alkaline peak comparable to the main peak had emerged around the injection point (Fig. 4b). Despite the appearance of the new alkaline band, the $\Delta F/F_m'$ profile did not change significantly, which means that the electron transport rate (proportional to $\Delta F/F_m'$ at a constant light intensity) remained high in the newly formed alkaline band. Within 3 h after the microinjection, the original alkaline peak (at 17 mm) had turned into an acidic band, while the new alkaline peak

had taken a stable position just to the left of the injection site. In addition, another alkaline peak appeared on the right-hand side of the pH profile (at 24 mm) (Fig. 4c). At the same time, the PSII quantum yield ($\Delta F/F_m'$) in the alkaline regions close to the injection site remained high. Similar rearrangements of pH and $\Delta F/F_m'$ profiles were observed in other experiments.

In conclusion, the experiments described here reveal a number of interesting features of the phenomenon of pH banding in *Chara* cells.

1. The short-term (minutes) effect of microinjection of NR-P peptide in an acidic band, namely the rapid increase in pH_o, is in line with an inhibition of the PM H^+-ATPase due to the competition between the peptide and the pump for binding to 14-3-3 protein [21].

2. In the longer term (hours), the pH profile became dynamic after peptide injection and the alkaline band, formed at the injection site, moved away from the site of injection and took up a stable position after a few hours just left of the site of injection (Fig. 4). This reorganization of closely positioned bands might be due to the disturbance of stationary band pattern by the artificially induced alkaline peak, leading to the achievement of a new stable state with interpeak distances appropriate for these cells. Such a rearrangement of pH profiles was observed, for example, after a dark–light transition, when some alkaline peaks were eliminated from the pH profile along with the enlargement of zones [12].

On the other hand, it is not excluded that the band shift was due to the slow spreading of NR-P along the cell. This is evidenced by the gradual flattening of the $\Delta F/F_m'$ profile, which was spread from the injection site.

The rate of pH band movement along the cell (about 1 mm/h) was much slower than the rate of cytoplasmic streaming (≥ 50 µm/sec or 180 mm/h), implying that the peptide was bound in the immobile cytoplasm or components and its mobility was restricted. Another explanation for the "slow" effect of peptide injection may be that 14-3-3 proteins play a role in the localization of proton pumps and/or proton channels [33]. Disturbance of this function might result in a time-dependent rearrangement of proteins in the membrane.

3. The correlation between the pH_o and $\Delta F/F_m'$ patterns is not absolute and can simply be disrupted by microinjection of NR-P. Thus, the PSII yield remained high in the newly formed alkaline band (peak at 11 mm), and the same disbalance of proton fluxes and linear electron transport was noted for the new alkaline peak positioned on the right-hand side of the profile (24 mm). Figure 5 shows normal and disrupted relations between pH_o and the quantum yield of PSII by plotting these quantities against each other. This presentation illustrates the breakdown of the correlation in cells injected with NR-P more clearly. Under normal conditions $\Delta F/F_m'$ declines with the increase in local pH (Fig. 5a), whereas in cell regions affected by NR-P treatment $\Delta F/F_m'$ is almost independent of pH (Fig. 5b).

An important question raised by the injection of the peptide is how $\Delta F/F_m'$ remains high in an alkaline band. One explanation is that the disarrangement of the concerted $\Delta F/F_m'$ and pH_o profiles after the injection of NR-P reflects the switching of the electron transport pathway from being CO_2-dependent to an alternative pathway like photo-assimilation. One possibility is that an increased
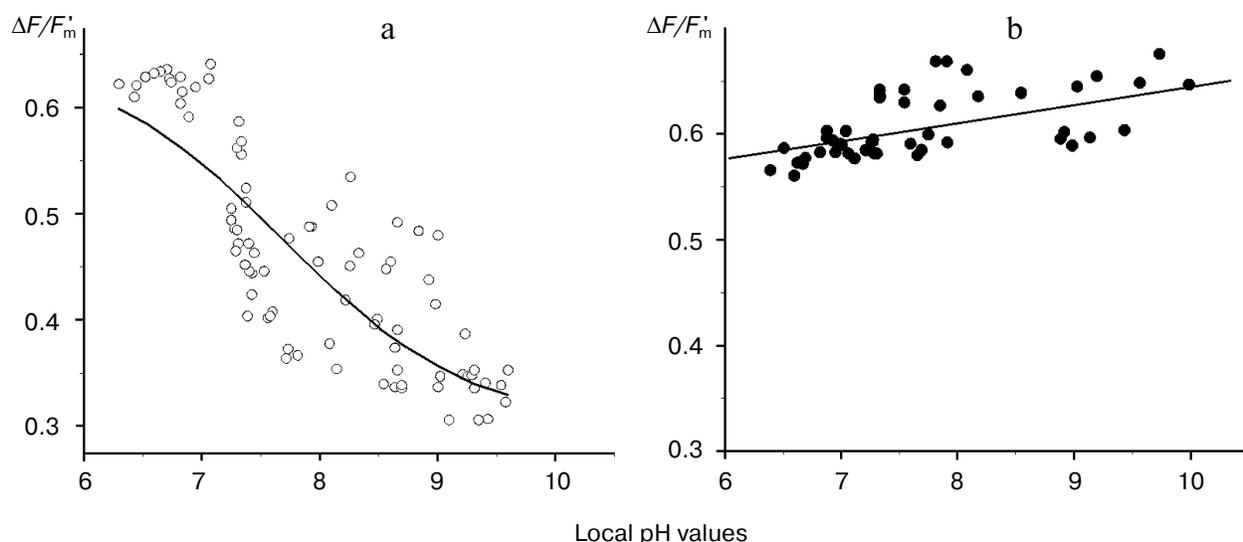
Fig. 5. Relations between local pH and $\Delta F/F_m'$ (photosynthetic rate indicator) in untreated *C. corallina* cells (a) and in cell regions affected by NR-P injection (b). Data in graphs were obtained on several cells illuminated at photon flux density of 20 µmol/sec per m². The results with NR-C treatment were similar to the control (a). A trend fitting of $\Delta F/F_m'$ vs. pH data with a sigmoid curve in panel (a) was made in the same way as explained in [13]. The straight line in panel (b) is a linear fit of data.

reduction of nitrite is involved. The activity of the enzyme that produces nitrite, nitrate reductase (NR), is controlled by phosphorylation dependent interaction with 14-3-3 proteins [34, 35]. Binding of 14-3-3 to NR completely inactivates the enzyme, but the NR-P peptide displaces 14-3-3, thereby activating NR (De Boer, unpublished results). NR is located in the cytosol of plant cells where it will be exposed to the injected peptide. Nitrite is subsequently reduced in the chloroplasts by nitrite reductase and the increased supply of nitrite can serve as an alternative acceptor for the non-cyclic electron flow in chloroplasts when CO_2 availability is limited.

In the case of NR-C injection, the disturbance of $\Delta F/F_m'$ and pH_o correlation cannot be easily revealed, because the injection of NR-C in the acid region did not produce a rise in pH_o and the photochemical yield remained high in that region. The correlation of pH_o and $\Delta F/F_m'$ remained undisturbed (data not shown).

In summary, our data suggest that the inhibition of the PM H⁺-pump by the peptide that binds 14-3-3 proteins leads to a disruption of a normal spatially coordinated functioning of linear electron transport in chloroplasts and the H⁺ transporting system of the plasma membrane. This may indicate the involvement of 14-3-3 proteins in the mechanism of the coordination of photosynthetic activity and membrane transport. The supposed role of 14-3-3 can be verified in further studies by determining if the inhibition of the PM H⁺-pump by treatments other than NR-P would affect the correlation of pH_o and $\Delta F/F_m'$.

REFERENCES

1. Tominaga, M., Kinoshita, T., and Shimazaki, K. (2001) *Plant Cell Physiol.*, **42**, 795-802.
2. Goh, C.-H., Dietrich, P., Steinmeyer, R., Schreiber, U., Nam, H.-G., and Hedrich, R. (2002) *Plant J.*, **32**, 623-630.
3. Serrano, E. E., Zeiger, E., and Hagiwara, S. (1988) *Proc. Natl. Acad. Sci. USA*, **85**, 436-440.
4. Vanselow, K. H., and Hansen, U.-P. (1989) *J. Membr. Biol.*, **110**, 175-187.
5. Bulychev, A. A., and Vredenberg, W. J. (1995) *Physiol. Plant.*, **94**, 64-70.
6. Plieth, C., Sattelmacher, B., and Hansen, U.-P. (1998) *Planta*, **207**, 52-59.
7. Plieth, C., Tabrizi, H., and Hansen, U.-P. (1994) *Physiol. Plant.*, **91**, 205-211.
8. Van Ginkel, L. C., and Prins, H. B. A. (1998) *Can. J. Bot.*, **76**, 1018-1024.
9. Baker, N. R., Oxborough, R., Lawson, T., and Morison, J. I. L. (2001) *J. Exp. Bot.*, **52**, 615-621.
10. Lucas, W. J., and Nuccitelli, R. (1980) *Planta*, **150**, 120-131.
11. Fisahn, J. M., and Lucas, W. J. (1995) *J. Membr. Biol.*, **147**, 275-281.
12. Bulychev, A. A., Polezhaev, A. A., Zykov, S. V., Pljusnina, T. Yu., Riznichenko, G. Yu., Rubin, A. B., Jantoss, W., Zykov, V. S., and Muller, S. C. (2001) *J. Theor. Biol.*, **212**, 275-294.
13. Bulychev, A. A., Cherkashin, A. A., Rubin, A. B., Vredenberg, W. J., Zykov, V. S., and Muller, S. C. (2001) *Bioelectrochemistry*, **53**, 225-232.
14. Bulychev, A. A., and Vredenberg, W. J. (2003) *Planta*, **218**, 143-151.
15. Hansen, U.-P., Moldaenke, C., Tabrizi, H., and Ramm, D. (1993) *Plant Cell Physiol.*, **34**, 681-695.
16. Smith, P. J. S., and Walker, N. A. (1985) *J. Membr. Biol.*, **83**, 193-205.
17. Yao, X., and Bisson, M. A. (1993) *Plant Physiol.*, **103**, 197-203.
18. Baunsgaard, L., Fuglsang, A. T., Jahn, T., Korthout, H., De Boer, A. H., and Palmgren, M. G. (1998) *Plant J.*, **13**, 661-671.
19. Kerkeb, L., Venema, K., Donaire, J. P., and Rodriguez-Rosales, M. P. (2002) *Physiol. Plant.*, **116**, 37-41.
20. Sehnke, P. C., DeLille, J. M., and Ferl, R. J. (2002) *Plant Cell*, **14**, S339-S354.
21. Bunney, T. D., van den Wijngaard, P. W. J., and De Boer, A. H. (2002) *Plant Mol. Biol.*, **50**, 1041-1051.
22. Tzivion, G., and Avruch, J. (2002) *J. Biol. Chem.*, **277**, 3061-3064.
23. Fuglsang, A. T., Visconti, S., Drumm, K., Jahn, T., Stensballe, A., Mattei, B., Jensen, O. N., Aducci, P., and Palmgren, M. G. (1999) *J. Biol. Chem.*, **274**, 36774-36780.
24. Kinoshita, T., and Shimazaki, K. (1999) *EMBO J.*, **18**, 5548-5558.
25. Kinoshita, T., and Shimazaki, K. (2001) *Plant Cell Physiol.*, **42**, 424-432.
26. Moorhead, G., Douglas, P., Cotelle, V., Harthill, J., Morrice, N., Meek, S., Deiting, U., Stitt, M., Scarabel, M., Aitken, A., and MacKintosh, C. (1999) *Plant J.*, **18**, 1-12.
27. Ichimura, T., Wakamiya-Tsuruta, A., Itagaki, C., Taoka, M., Hayano, T., Natsume, T., and Isobe, T. (2002) *Biochemistry*, **41**, 5566-5572.
28. Bunney, T. D., van Walraven, H. S., and De Boer, A. H. (2001) *Proc. Natl. Acad. Sci. USA*, **98**, 4249-4254.
29. Booij, P. P., Roberts, M. R., Vogelzang, S. A., Kraayenhof, R., and De Boer, A. H. (1999) *Plant J.*, **20**, 673-683.
30. Goh, C.-H., Schreiber, U., and Hedrich, R. (1999) *Plant Cell Environ.*, **22**, 1057-1070.
31. Shimmen, T., and Yamamoto, A. (2002) *Plant Cell Physiol.*, **43**, 980-983.
32. De Boer, A. H. (1997) *Trends Plant Sci.*, **2**, 60-66.
33. Rajan, S., Preisig-Muller, R., Wischmeyer, E., Nehring, R., Hanley, P. J., Renigunta, V., Musset, B., Schlichthorl, G., Derst, C., Karschin, A., and Daut, J. (2002) *J. Physiol.*, **545**, 13-26.
34. MacKintosh, C., Douglas, P., and Lillo, C. (1995) *Plant Physiol.*, **107**, 451-457.
35. Huber, S. C., MacKintosh, C., and Kaiser, W. M. (2002) *Plant Mol. Biol.*, **50**, 1053-1063.